Supporting Information (SI)

Sequential Donor–Acceptor Dual Modulation in Conjugated Microporous Polymers Enables Efficient Photocatalytic Synthesis of Symmetric Ureas, Benzothiazoles and Functionalized Indoles

Soumitra Sau, Sibu Manna[#], Suman Karmakar[#], Sayan Roy[$], Bipul Mondal[$], Suman Joardar and Suman Kalyan Samanta*

Department of Chemistry, Indian Institute of Technology Kharagpur, Kharagpur 721302, India. E-mail: sksamanta@chem.iitkgp.ac.in

1. Experimental Section

1.1. Materials and Methods. All the chemicals and reagents were purchased from commercial sources and used directly as raw materials without further treatment. Thin-layer chromatography (TLC) on silica gel GF254 was used for the determination of R_f values and the visualization was performed by irradiation with a UV lamp at 254 nm. Column chromatography was performed on Merck silica gel (100-200 mesh) with eluent as mentioned. ^{1}H (500 MHz) and ^{13}C (125 MHz) NMR spectra were recorded in a Bruker advance-500 NMR spectrometer in deuterated solvent at ambient temperature (300 K). Chemical shifts are reported in ppm (δ) relative to tetramethylsilane (TMS) as the internal standard ($CDCl_3$ δ 7.26 ppm for ^{1}H and 77.0 ppm for ^{13}C). Solid state ^{13}C CPMAS NMR spectra were recorded in a Bruker Ultrashield-500 NMR spectrometer. Fourier transform infrared spectra (FTIR, 4000-600 cm^{-1}) were performed on Nicolet 6700 FT-IR spectrometer (Thermo Fischer) Instrument, the wavenumbers of the recorded IR signals are reported in cm^{-1}. Thermogravimetric analyses (TGA) were performed on a Pyris Diamond TG DTA (PerkinElmer) instrument. Elemental analysis (C, H, N, and S) of the CMPs was carried out using a Thermo Scientific FlashSmart CHNS analyzer. The morphology of the as-synthesized D–A CMPs was examined by scanning electron microscopy (SEM, ZEISS SUPRA 40). Samples were prepared by placing the powdered polymers on gold stubs using double-sided carbon tape. Transmission Electron Microscopy (TEM, JEOL F200) operated at 200 kV, was used to investigate surface morphology along with High-Resolution TEM (HRTEM) images. UV–Vis–NIR diffuse reflectance spectra (DRS) were recorded on a Cary 5000 UV–Vis–NIR spectrophotometer (Agilent). Powder X-ray diffraction (PXRD) patterns of the polymer samples were obtained on a Bruker AXS D8 Advance SWAX diffractometer using Cu Kα radiation (λ = 0.15406 nm). The N_2 adsorption/desorption isotherms of the sample were recorded on a Quantachrome Autosorb iQ2 surface area and pore size analyzer at 77 K. UV–visible absorption spectra were recorded using a Shimadzu UV-2550 UV–vis spectrophotometer. Reactive oxygen species (ROS) trapping experiments were performed under photocatalytic conditions. For superoxide radical ($O_2^{\bullet-}$) detection, 5 mg of the photocatalyst and 5 mg of *N,N,N′,N′-tetramethyl-p-phenylenediamine* (TMPD) were dispersed in 3 mL of air-saturated CH_3CN, further purged with O_2, and irradiated with a 24 W white LED under stirring. After the desired irradiation time, the reaction mixture was filtered through a syringe filter, and the filtrate was analyzed by UV–vis spectroscopy. For singlet oxygen ($^1O_2$) trapping, 1 mg of the photocatalyst was added to 5 mL of a 25 μM solution of diphenylisobenzofuran (DPBF) in CH_3CN under air atmosphere and irradiated with a 24 W white LED under continuous stirring. The generation of $^1O_2$ was monitored by the time-dependent decrease in the characteristic absorption of DPBF using UV–vis spectroscopy. EPR spectra were recorded on a Bruker ELEXSYS 580 spectrometer. For ROS trapping experiments, the measurement parameters were as follows: modulation frequency = 100 kHz and modulation amplitude = 5 G. The samples were prepared by dispersing 1 mg of photocatalyst in 1 mL of 0.1 M air-saturated methanol solution containing 5,5-dimethyl-1-pyrroline-N-oxide (DMPO) for $O_2^{\bullet-}$ detection or 2,2,6,6-tetramethylpiperidine (TEMP) for $^1O_2$ trapping. Density functional theory (DFT) calculations were performed using the Gaussian 09W program package. Adsorption energies were evaluated using a fragment-based DFT

approach, in which representative oligomeric units were extracted from the CMP backbone. Geometry optimizations and energy calculations were carried out using the B3LYP functional with the 6-31G basis set. It should be noted that such cluster models do not fully capture long-range π-conjugation, pore-confinement effects, or collective electronic interactions inherent to extended CMP networks. Consequently, the calculated adsorption energies are intended to provide qualitative insights into relative adsorption trends, rather than precise quantitative values of absolute interaction strengths.

1.2. Electrochemical measurements

Electrochemical experiments were performed using a CH Instruments electrochemical workstation in a standard three-electrode setup under illumination from a 20 W white LED. The working electrodes were prepared by dispersing 2 mg of the dried CMP sample with 0.5 mg of polyvinylidene fluoride (PVDF) and 50 μL of ethanol to form a uniform slurry. The slurry was coated onto fluorine-doped tin oxide (FTO) glass substrates (active area: 1 cm^2) and dried at 80 °C for 1 h to remove residual solvent. An aqueous 0.2 M Na_2SO_4 solution served as the supporting electrolyte.

Photocurrent measurements, Mott–Schottky analysis, and electrochemical impedance spectroscopy (EIS) were carried out using the CMP-coated FTO as the working electrode, a platinum wire as the counter electrode, and an Ag/AgCl (3 M KCl) electrode as the reference. Transient photocurrent responses were measured at 0.3 V versus Ag/AgCl under chopped light illumination. Flat-band potentials (vs. Ag/AgCl) were determined from the extrapolated tangent of the Mott–Schottky plots collected at frequencies of 1250, 1500, and 1750 Hz.

1.3. Determination of Quantum Yield:

Determination of the photon flux (I_0): The photon flux of the incident light source was determined by chemical actinometry using indolyl fulgide, following a previously reported method with appropriate adaptation by Mondal *et al*. (*J. Am. Chem. Soc.* **2024,** *146* (33), 23376). The actinometric principle is based on the light-induced, reversible photoisomerization of the fulgide between its open (1Z) and closed (1C) forms, as illustrated schematically below.

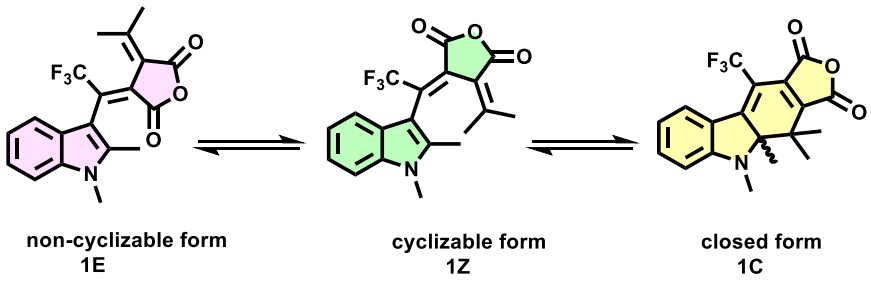

A freshly prepared solution of compound 1 (3 mL, 1.0×10^{-4} M) in toluene was placed in a quartz fluorescence cuvette equipped with a magnetic stir bar to maintain uniform mixing

during irradiation. Upon exposure to blue light (456 ± 10 nm), UV–vis absorption spectra were recorded at defined time intervals. The progress of the photoisomerization reaction was monitored by tracking the change in absorbance at 427 nm, expressed as ($A_0 - A$) as a function of irradiation time (t).

The photon flux associated with the conversion of the 1Z isomer to the corresponding 1C isomer was calculated using Equation (1):

$$\mathbf{I_0} = \frac{\Delta A}{t}\frac{V}{\varepsilon d \Phi} \quad \text{..... (1)}$$

where I_0 is the photon flux of the incident light (Einsteins s^{-1}), ΔA represents the increase in absorbance corresponding to the formation of the closed isomer over time t, V is the solution volume (mL), ε denotes the molar absorption coefficient of the 1Z isomer at 427 nm (M^{-1} cm^{-1}), d is the optical path length of the cuvette (cm), and Φ is the quantum yield of the photoisomerization process.

The UV–vis spectral evolution of indolyl fulgide under blue light irradiation (456 ± 10 nm), along with the corresponding time-dependent absorbance changes at 427 nm, are presented below.

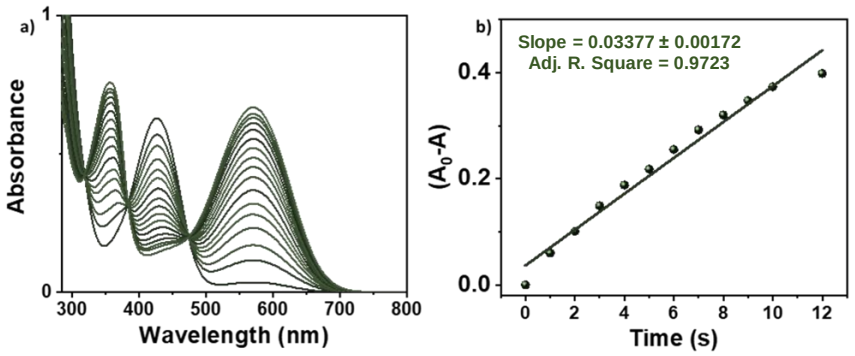

Incident Light	Slope (ΔA/t)	Sample Volume (cm^3)	Photon Flux (Einstein s^{-1})
456 ± 10 nm	**0.03377 ± 0.00172**	**3**	**2.05×10^{-7}**

Determination of the apparent quantum yield (AQY):

The apparent quantum yield (AQY, Φ) of the photochemical reaction was calculated using the equation (2)

$$\mathbf{AQY} = \frac{n_{product}}{Flux \times t} \quad \text{..... (2)}$$

where $n_{product}$ is the number of moles of product formed, t is the irradiation time in seconds, the photon flux is the number of incident photons per second (Einstein·s^{-1}).

1.3.1. Determination of AQY for the photocatalytic synthesis of *N,N*-diphenylurea from aniline and CS_2 :

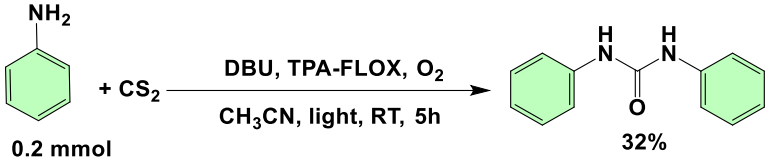

$$\Phi = \frac{0.2 \times 0.32 \times 10^{-3}\, mol}{2.05 \times 10^{-7}\, E.s^{-1} \times (300 \times 60)s} \times 100 = 0.017$$

1.3.2 Determination of AQY for the photocatalytic C-3 thiocyanation of indoles:

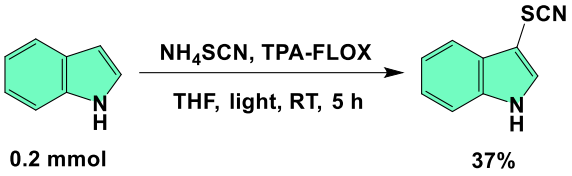

$$\Phi = \frac{0.2 \times 0.37 \times 10^{-3}\, mol}{2.05 \times 10^{-7}\, E.s^{-1} \times (300 \times 60)s} \times 100 = 0.02$$

1.3.3. Determination of AQY for the photocatalytic synthesis of 2-phenylbenzo[d]thiazole:

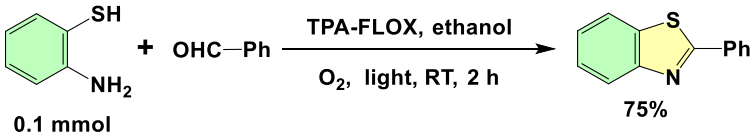

$$\Phi = \frac{0.1 \times 0.75 \times 10^{-3}\, mol}{2.05 \times 10^{-7}\, E.s^{-1} \times (120 \times 60)s} \times 100 = 0.051$$

Synthetic Procedure

Synthesis of FLOX-Br2

In a 100 mL round-bottom flask, 2,7-dibromo-9H-fluoren-9-one (3.38 g, 0.01 mol), sodium hydroxide (0.60 g, 0.015 mol), and methoxyamine hydrochloride (1.25 g, 0.015 mol) were dissolved in ethanol (30 mL). The reaction mixture was refluxed for 12 h, then poured into ice–water (20 mL) to yield a pale-yellow precipitate. The solid was collected by filtration, washed thoroughly with cold water, and dried. Recrystallization from hot methanol–water afforded pure FLOX-Br_2 as pale-yellow crystals (3.31 g, 90% yield), which was directly used in the subsequent step (**Scheme S1**). ^{1}H NMR (400 MHz, $CDCl_3$) (**Figure S1**): δ 8.41 (s, 1H), 7.91 (s, 1H), 7.59 (d, 1H), 7.51–7.28 (m, 3H), 4.26 (s, 3H) ppm; ^{13}C NMR (125 MHz, $CDCl_3$) (**Figure S2**): δ 149.83, 138.97, 137.86, 136.93, 133.65, 132.61, 131.93, 131.52, 124.80, 121.95, 121.12, 120.99, 63.84 ppm; HRMS: 364.9051 (calc.); 364.9055 (obtained). FTIR (**Figure S3**): 2940, 1617, 1434,1267, 1157, 1107, 1063, 983, 888, 808, 750, 699, 656, 604 and 474 cm^{-1}.

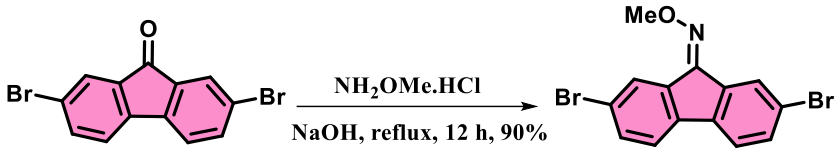

Scheme S1. Synthetic procedure for monomer FLOX-Br2.

Synthesis of D-A CMPs:

Synthesis of TPA-FLO:

A mixture of tris(4-(4,4,5,5-tetramethyl-1,3,2-dioxaborolan-2-yl)phenyl)amine (305 mg, 0.49 mmol), 2,7-dibromo-9H-fluoren-9-one (250 mg, 0.74 mmol), $Pd(PPh_3)_4$ (29 mg, 5 mol%), and K_2CO_3 (1.08 g, 7.84 mmol) was added to a 100 mL two-neck round-bottom flask under an argon atmosphere. A degassed solvent mixture of toluene (12 mL) and water (4 mL) was introduced, and the reaction mixture was purged with argon for 30 minutes. The mixture was then stirred vigorously at 95 °C for 4 days. After cooling, the resulting solid was collected by filtration and washed thoroughly with water, methanol, and chloroform. Further purification was performed by Soxhlet extraction, using methanol, acetone, and chloroform sequentially, with each solvent used for one day. The final product was dried under vacuum to yield an orange polymer (220 mg, 87% yield). Characterization data: FT-IR (cm^{-1}): 1711, 1595, 1508, 1465, 1290, 1182, 819, 790, 732, 499; ^{13}C CP-MAS NMR (ppm): ~191, ~147, ~142, ~136–118; TGA: 5% weight loss at 405 °C; elemental analysis: found C 87.93%, H 4.30%, N 1.92%; calculated C 87.78%, H 4.27%, N 1.80%.

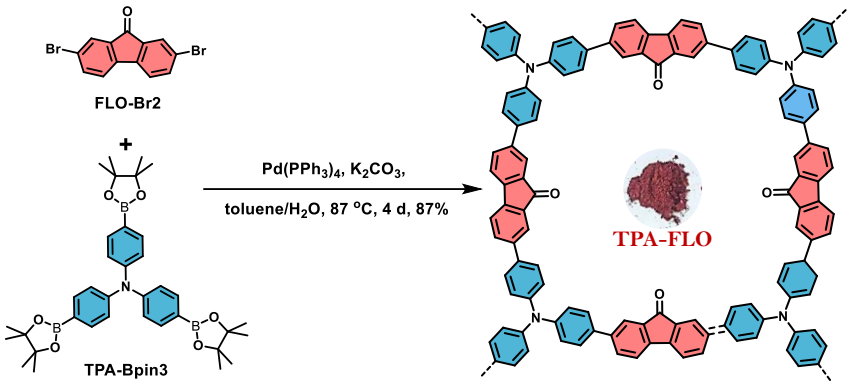

Scheme S2. Synthetic procedure for **TPA-FLO** (inset: photograph showing the polymer's color).

Synthesis of TPA-FLOX: A mixture of tris(4-(4,4,5,5-tetramethyl-1,3,2-dioxaborolan-2-yl)phenyl)amine (340 mg, 0.543 mmol), 2,7-dibromo-9H-fluoren-9-one O-methyl oxime (300 mg, 0.817 mmol), $Pd(PPh_3)_4$ (32 mg, 5 mol%), and K_2CO_3 (1200 mg, 8.688 mmol) was added to a 100 mL two-neck round-bottom flask under an argon atmosphere. A degassed solvent mixture of toluene (12 mL) and water (4 mL) was introduced, and the reaction mixture was purged with argon for 30 minutes. The mixture was then stirred vigorously at 95 °C for 4 days. After cooling, the resulting solid was collected by filtration and washed thoroughly with water, methanol, and chloroform. Further purification was performed by Soxhlet extraction, using methanol, acetone, and chloroform sequentially, with each solvent used for one day. The final product was dried under vacuum to yield an orange polymer (290 mg, 95% yield). Characterization data: FT-IR (cm^{-1}): 1600, 1507, 1456, 1041, 991, 814, 509; ^{13}C CP-MAS NMR (ppm): ~151, ~147, ~139, ~131–117, ~63 ; TGA: 5% weight loss at 362 °C; elemental analysis: found C 83.258%, H 4.818%, N 5.664%; calculated C 83.12%, H 4.88%, N 6.46%.

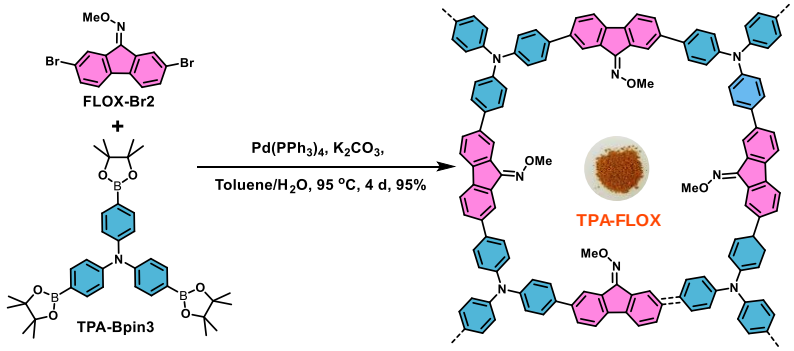

Scheme S3. Synthetic procedure for **TPA-FLOX** (inset: photograph showing the polymer's color).

Synthesis of TRZ-FLOX: A mixture of 2,4,6-tris(4-(4,4,5,5-tetramethyl-1,3,2-dioxaborolan-2-yl)phenyl)-1,3,5-triazine (350 mg, 0.509 mmol), 2,7-dibromo-9H-fluoren-9-one O-methyl oxime (281 mg, 0.766 mmol), $Pd(PPh_3)_4$ (30 mg, 5 mol%), and K_2CO_3 (1122 mg, 8.146 mmol) was added to a 100 mL two-neck round-bottom flask under an argon atmosphere. A degassed solvent mixture of toluene (12 mL) and water (4 mL) was introduced, and the reaction mixture was purged with argon for 30 minutes. The mixture was then stirred vigorously at 95 °C for 4 days. After cooling, the resulting solid was collected by filtration and washed thoroughly with water, methanol, and chloroform. Further purification was performed by Soxhlet extraction, using methanol, acetone, and chloroform sequentially, with each solvent used for one day. The final product was dried under vacuum to yield an orange polymer (285 mg, 90% yield). Characterization data: FT-IR (cm^{-1}): 1570, 1475, 1374, 1272, 1243, 1178, 1105, 1018, 887, 800, 700, 640, 545; ^{13}C CP-MAS NMR (ppm): ~170, ~151, ~137, ~131–117, ~63; TGA indicated 5% weight loss at 335 °C; elemental analysis: found C 81.37%, H 4.961%, N 8.796%; calculated C 81.27%, H 4.55%, N 9.03%.

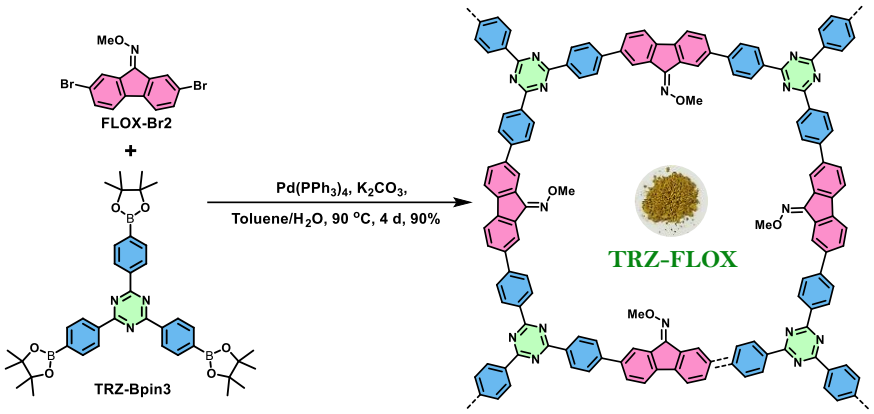

Scheme S4. Synthetic procedure for **TRZ-FLOX** (inset: photograph showing the polymer's color).

2. Characterizations:

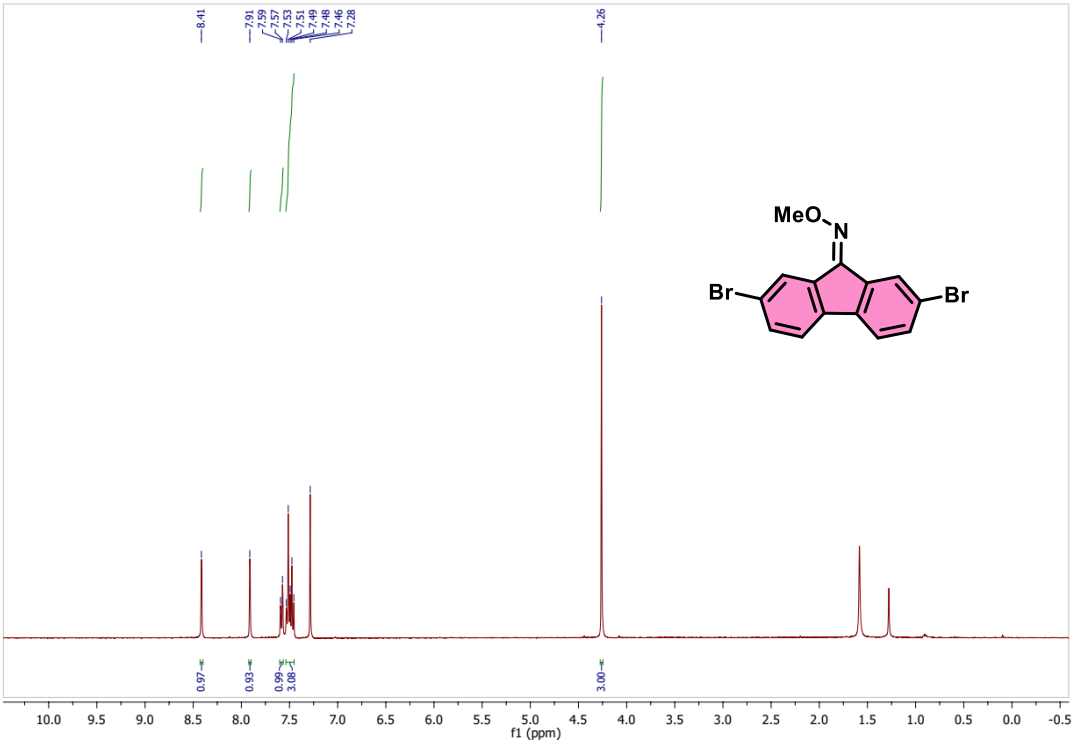

Figure S1. ^{1}H NMR spectrum of FLOX-Br2.

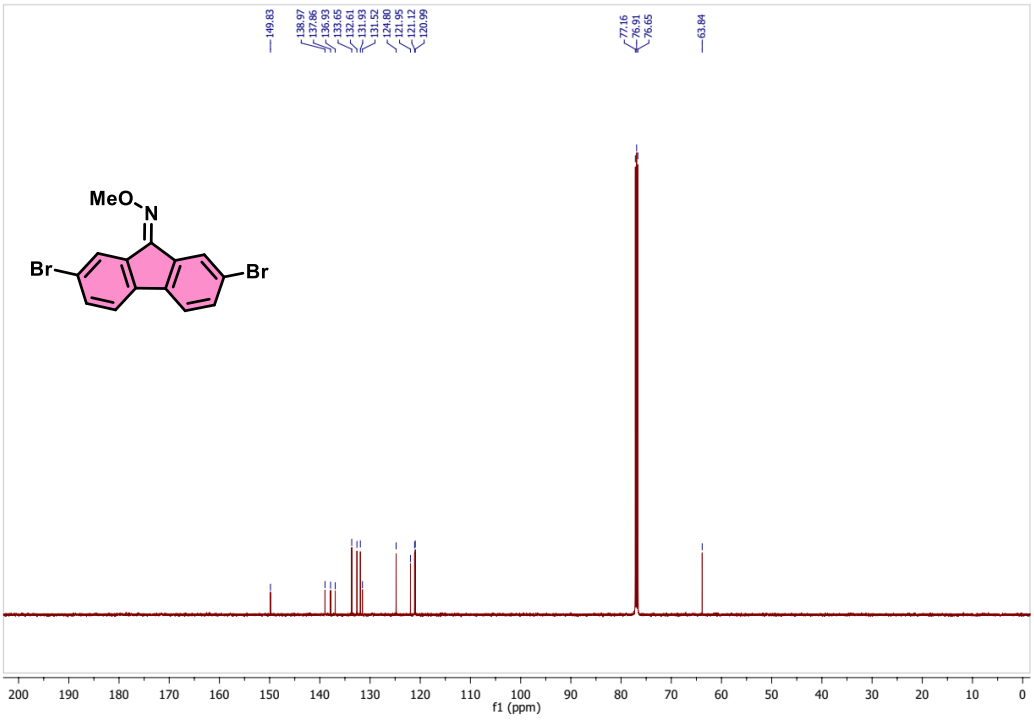

Figure S2. ^{13}C NMR spectrum of FLOX-Br2.

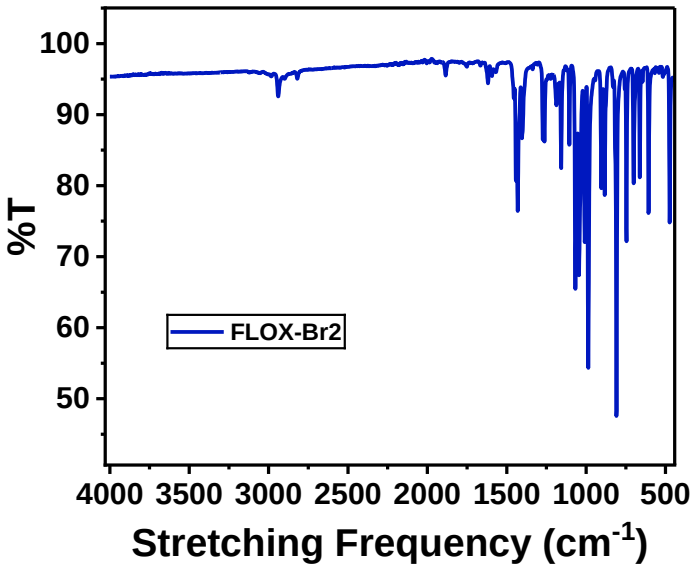

Figure S3. FTIR spectrum of FLOX-Br2.

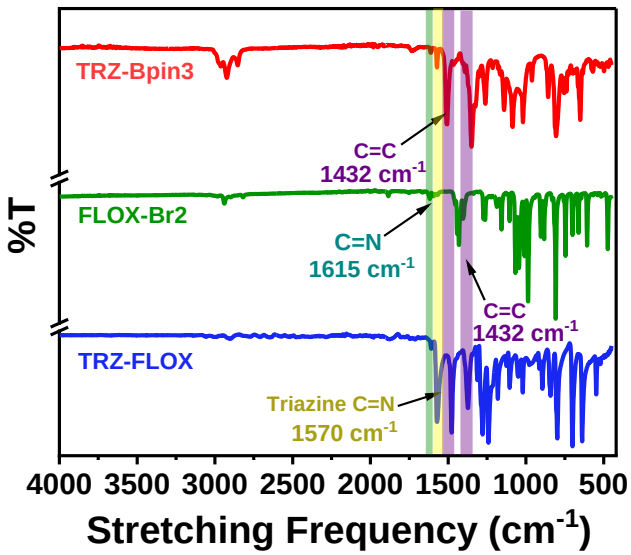

Figure S4. FT-IR spectra of monomer TRZ-Bpin3 (green), monomer FLOX-Br2 (pink) and polymer **TRZ-FLOX** (blue).

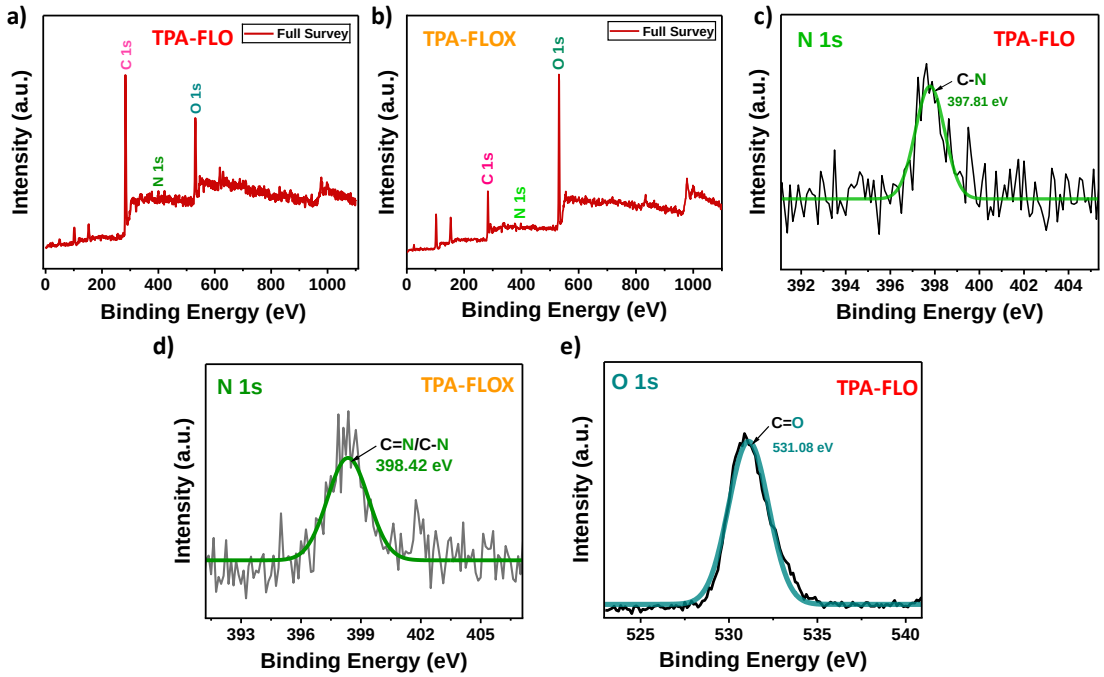

Figure S5. XPS full survey spectra of a) **TPA-FLO** and b) **TPA-FLOX**; high-resolution N 1s spectra of c) **TPA-FLO** and d) **TPA-FLOX**; e) high-resolution O 1s spectrum of **TPA-FLO**.

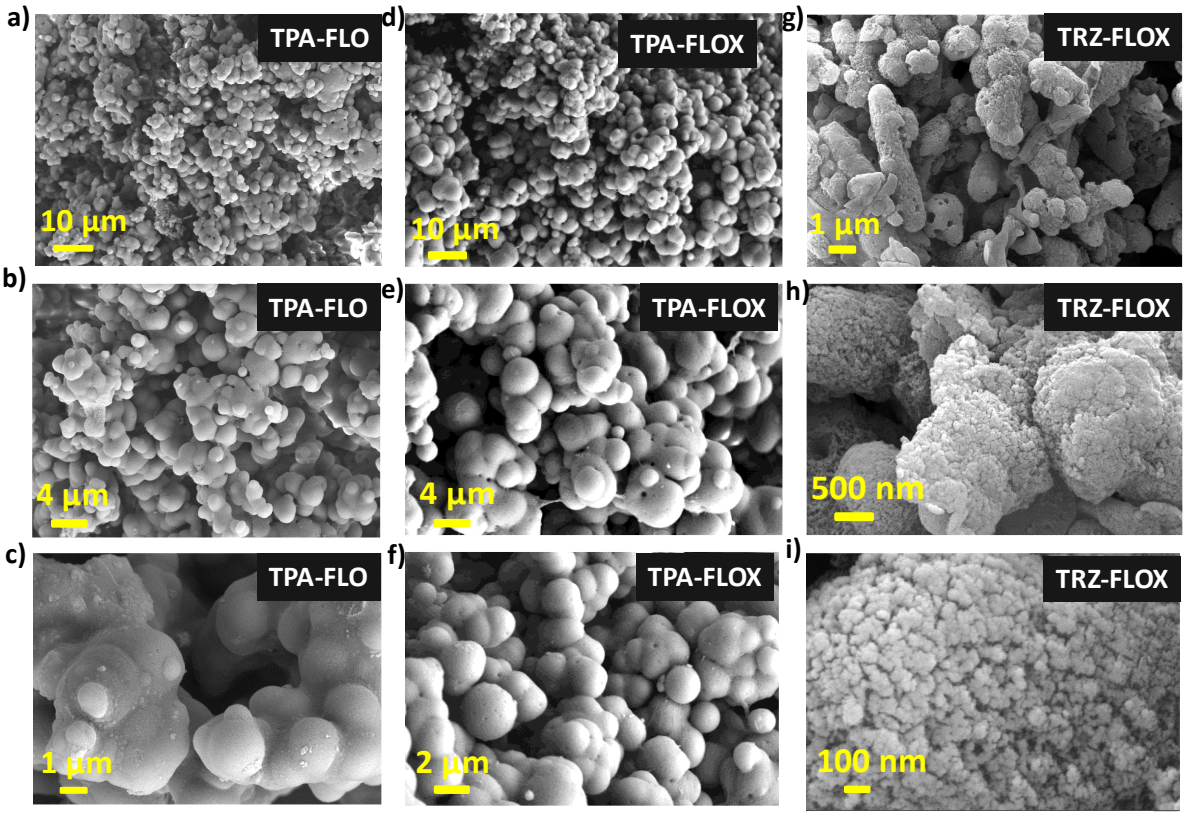

Figure S6. SEM images of a-c) **TPA-FLO**, d-f) **TPA-FLOX**, and g-i) **TRZ-FLOX** at different magnifications.

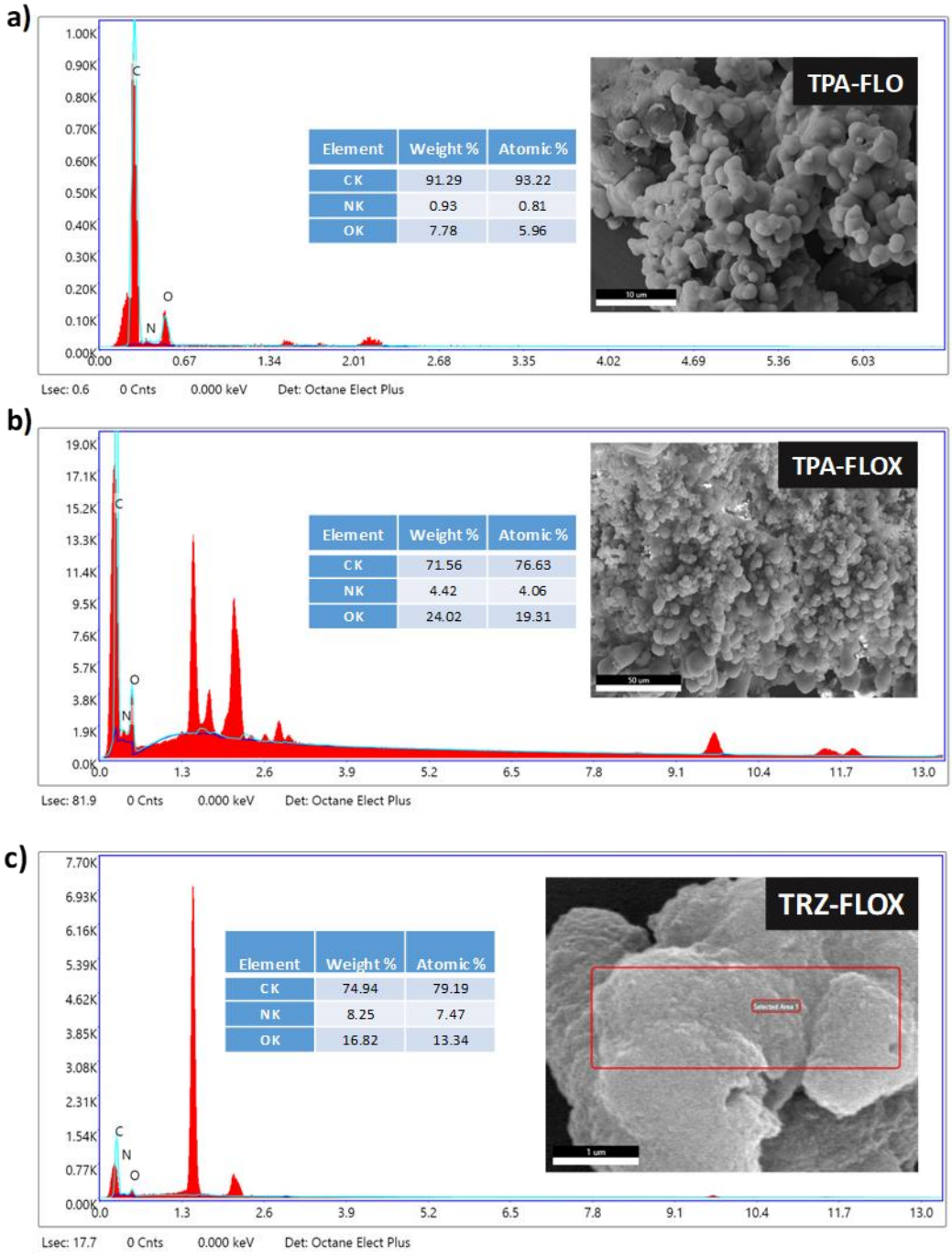

Figure S7. Energy dispersive X-ray (EDX) analysis of a) **TPA-FLO**, b) **TPA-FLOX**, and c) **TRZ-FLOX** coupled with scanning electron microscopy; inset: tabular representation of different elements in weight% and atomic% present in the polymer.

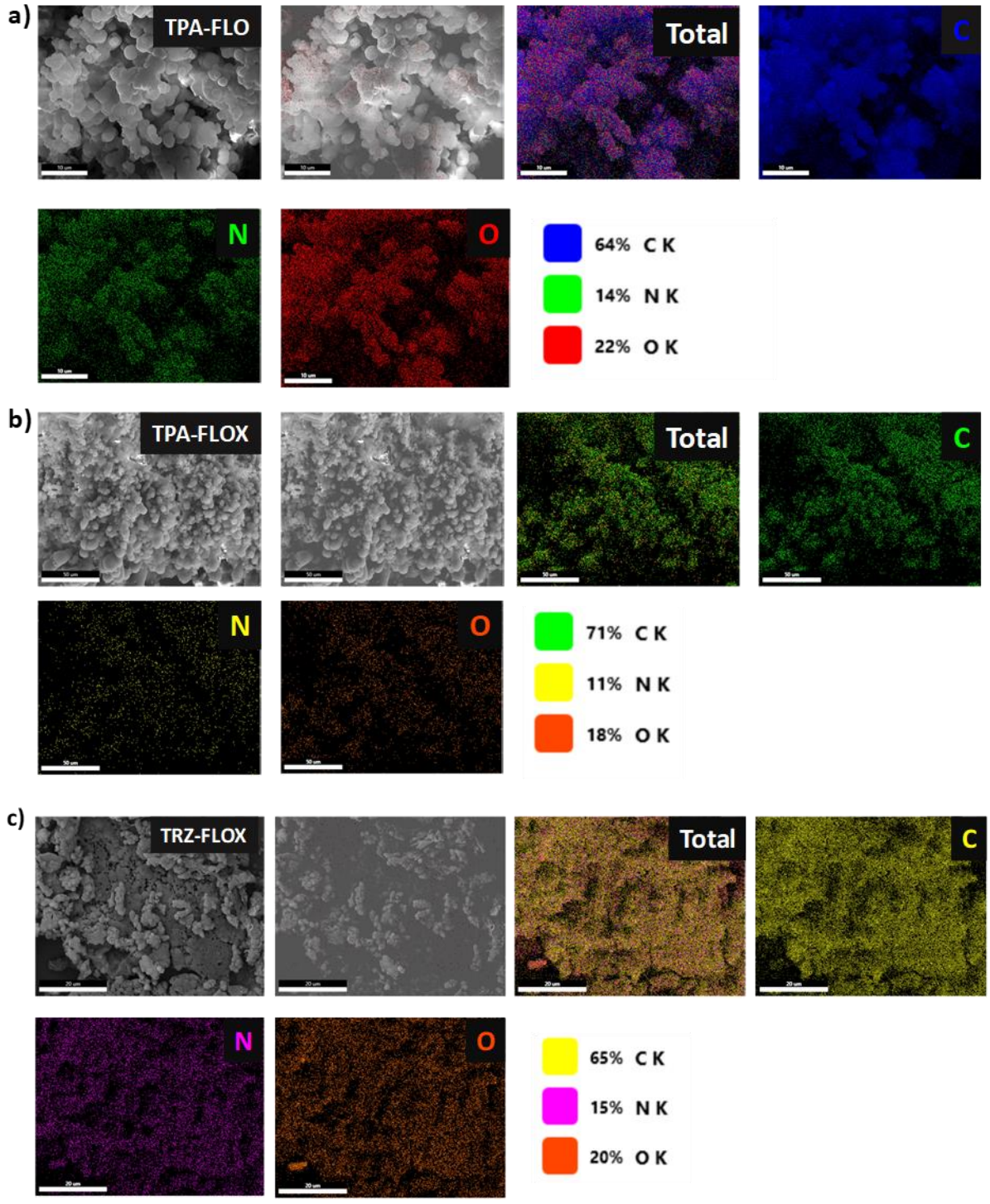

Figure S8. Elemental mapping analysis of a) **TPA-FLO**, b) **TPA-FLOX** and c) **TRZ-FLOX**.

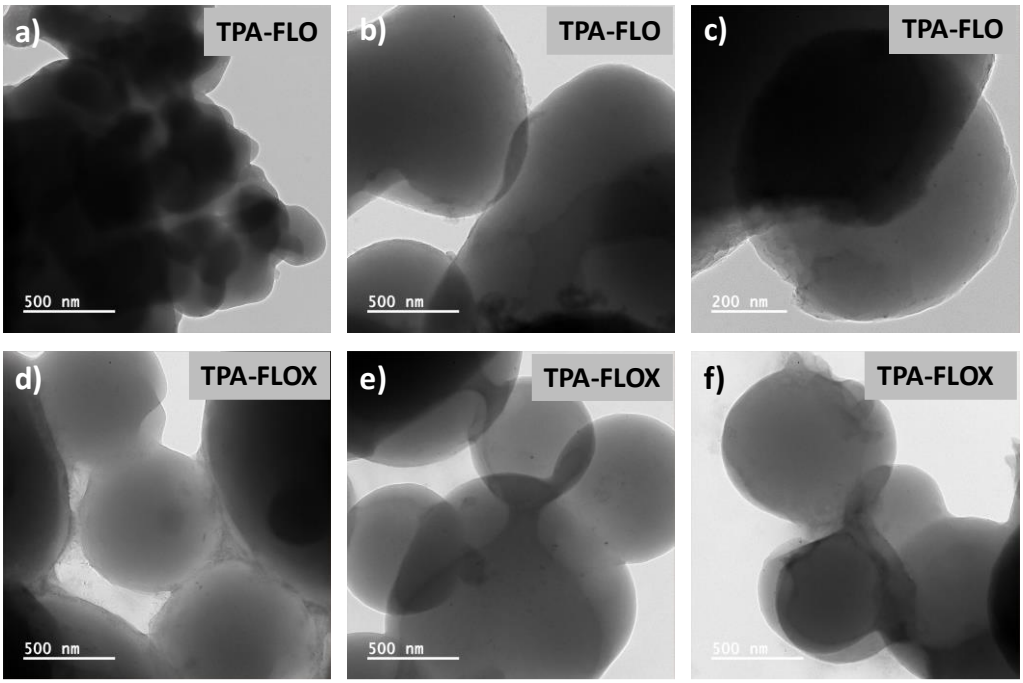

Figure S9. TEM images of a-c) **TPA-FLO** and d-f) **TPA-FLOX**.

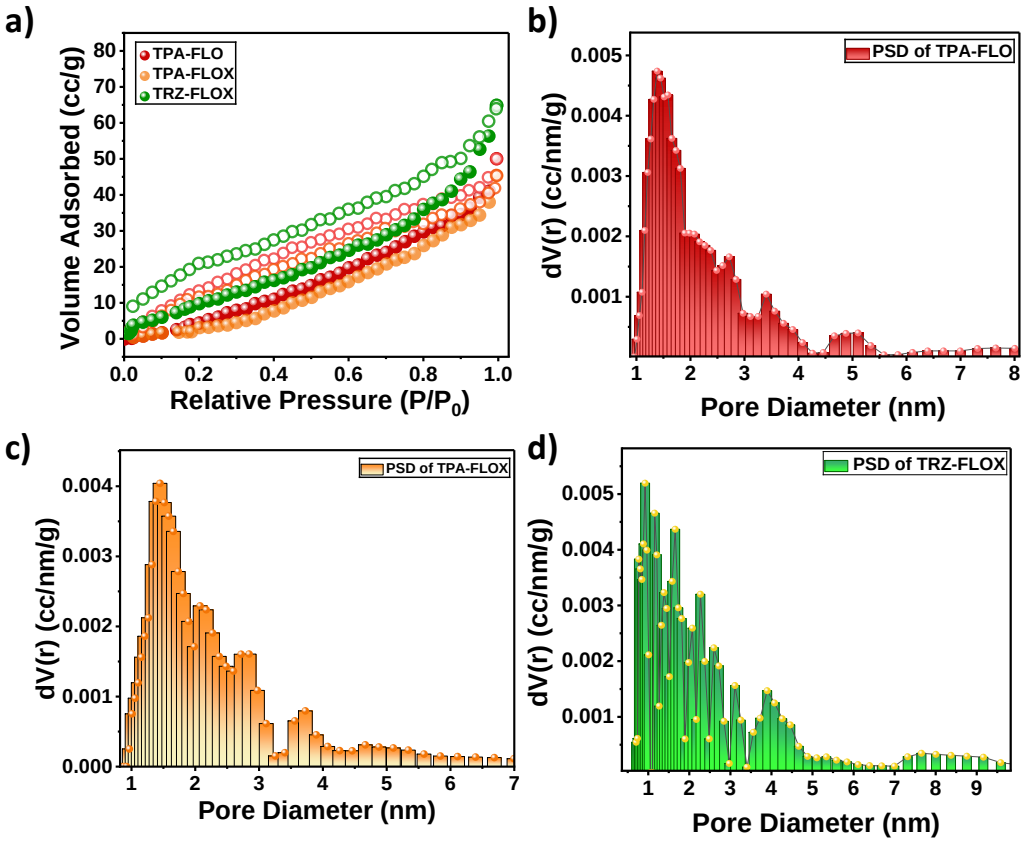

Figure S10. a) Nitrogen adsorption–desorption isotherms of the CMPs measured at 77 K; NLDFT-derived pore size distribution curve of b) **TPA-FLO**, c) **TPA-FLOX**, and d) **TRZ-FLOX**.

Table S1. BET surface area, pore volume, and average pore diameter of the CMPs.

CMPs	BET surface area (m^2/g)	NLDFT-derived pore volume (cc/g)	Pore Diameter (nm)
TPA-FLO	30	0.082	1.38
TPA-FLOX	27	0.056	1.45
TRZ-FLOX	43	0.086	0.92

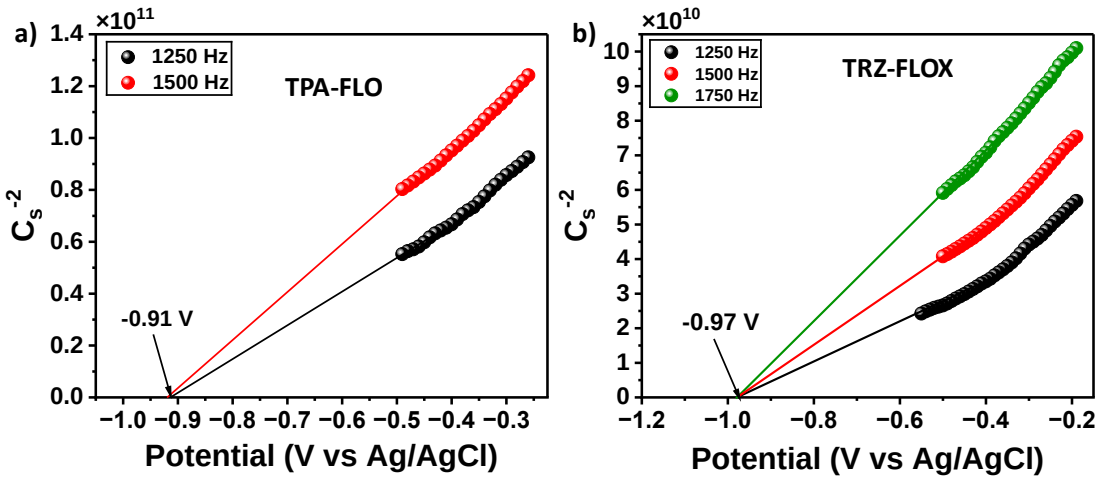

Figure S11. Mott–Schottky plots of a) **TPA-FLO** and b) **TRZ-FLOX** recorded at different frequencies.

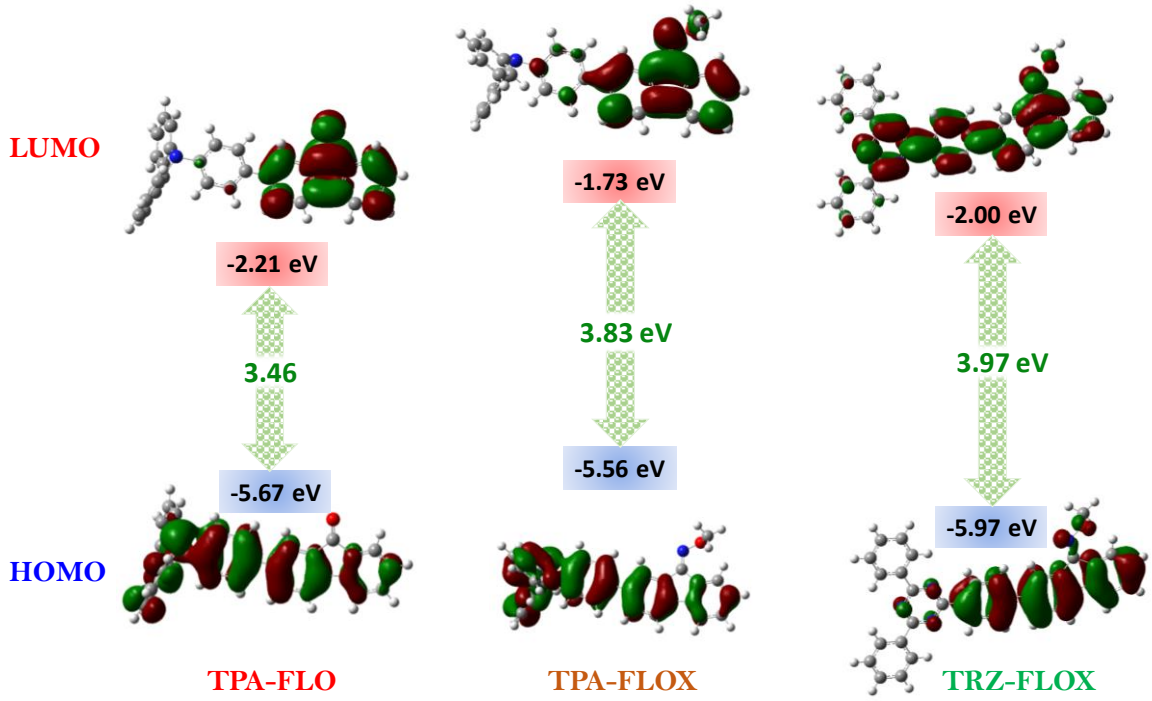

Figure S12. Electronic structures of the HOMO–LUMO orbitals and the corresponding relative energy levels of the fragment units of **TPA-FLO**, **TPA-FLOX**, and **TRZ-FLOX**, as obtained from DFT calculations.

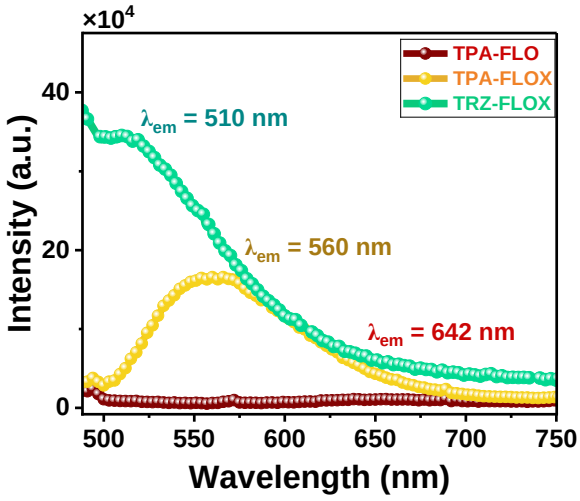

Figure S13. Steady-state PL spectra of the CMPs.

3. Photocatalytic Applications

Table S2. Comparison of photocatalytic performance of **TPA-FLOX** in photosynthesis of symmetric ureas.

Entry	Photocatalyst	Catalyst type	Light source	Time (h)	Yield (%)	Reference
1	**Rh-B** (10.0 mol%)	Homogeneous	10 W Blue LED	12	88	L. Duan *et al.*,[1] Molecular Catalysis 564 (2024) 114344
2	**Eosin Y** (10.0 mol%)	Homogeneous	10 W Blue LED	12	51	L. Duan *et al.*,[1] Molecular Catalysis 564 (2024) 114344
3	**Rose Bengal** (10.0 mol%)	Homogeneous	10 W Blue LED	12	20	L. Duan *et al.*,[1] Molecular Catalysis 564 (2024) 114344
4	**[Ru (BPY)3] Cl2•6H2O** (10.0 mol%)	Homogeneous	10 W Blue LED	12	63	L. Duan *et al.*,[1] Molecular Catalysis 564 (2024) 114344
5	**TPA-FLOX** (8 mg)	Heterogeneous	25W White LED	10	90	This work

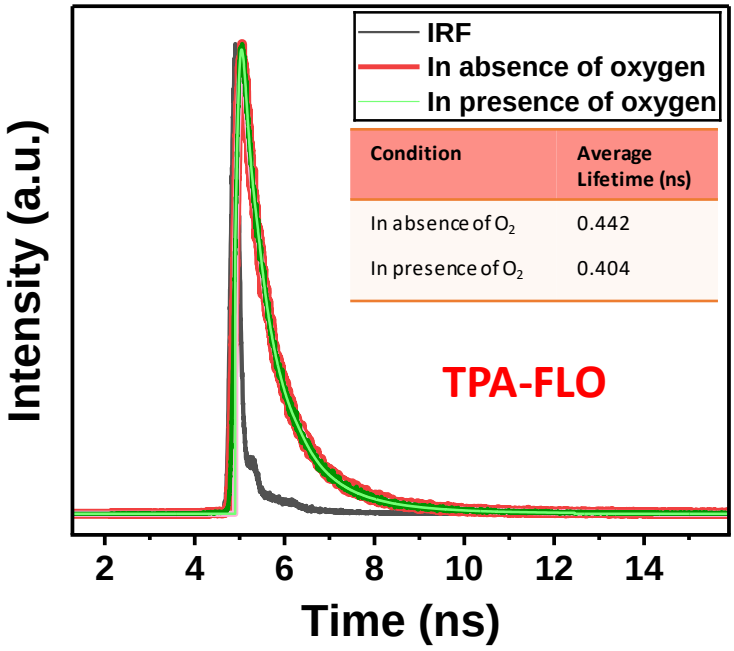

Figure S14. TRPL spectra of **TPA-FLO** in absence and presence of oxygen.

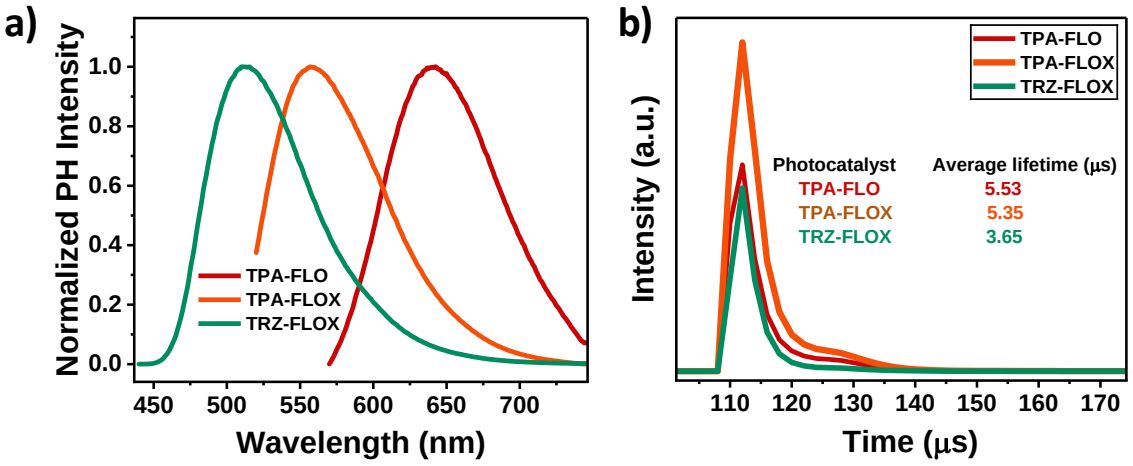

Figure S15. a) Normalized phosphorescence (PH) spectra of the CMPs recorded at 300 K and b) Phosphorescence decay profiles of the polymers monitored at the respective emission maxima of each compound.

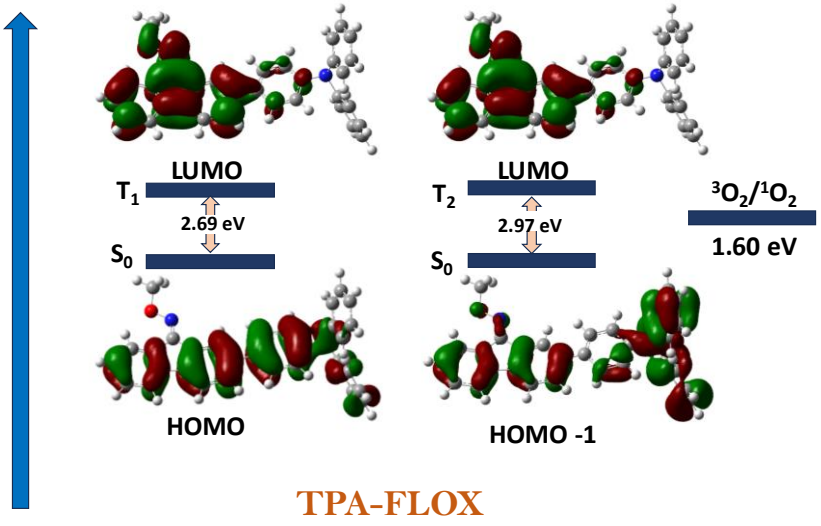

Figure S16. Energy-level diagram illustrating the calculated S_0, T_1, and T_2 states of **TPA-FLOX** and their relation to the $^3O_2 \rightarrow {}^1O_2$ energy gap (1.60 eV), supporting the feasibility of $^1O_2$ generation via energy transfer.

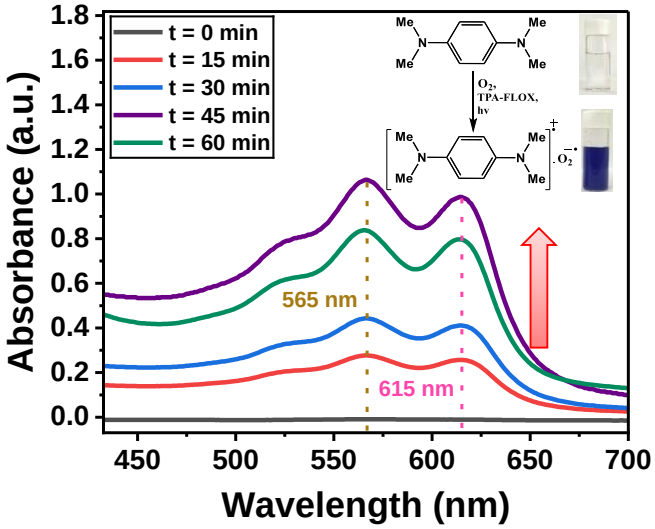

Figure S17. UV–vis absorption spectra of the TMPD cationic radical generated in the presence of **TPA-FLOX**, recorded as a function of time.

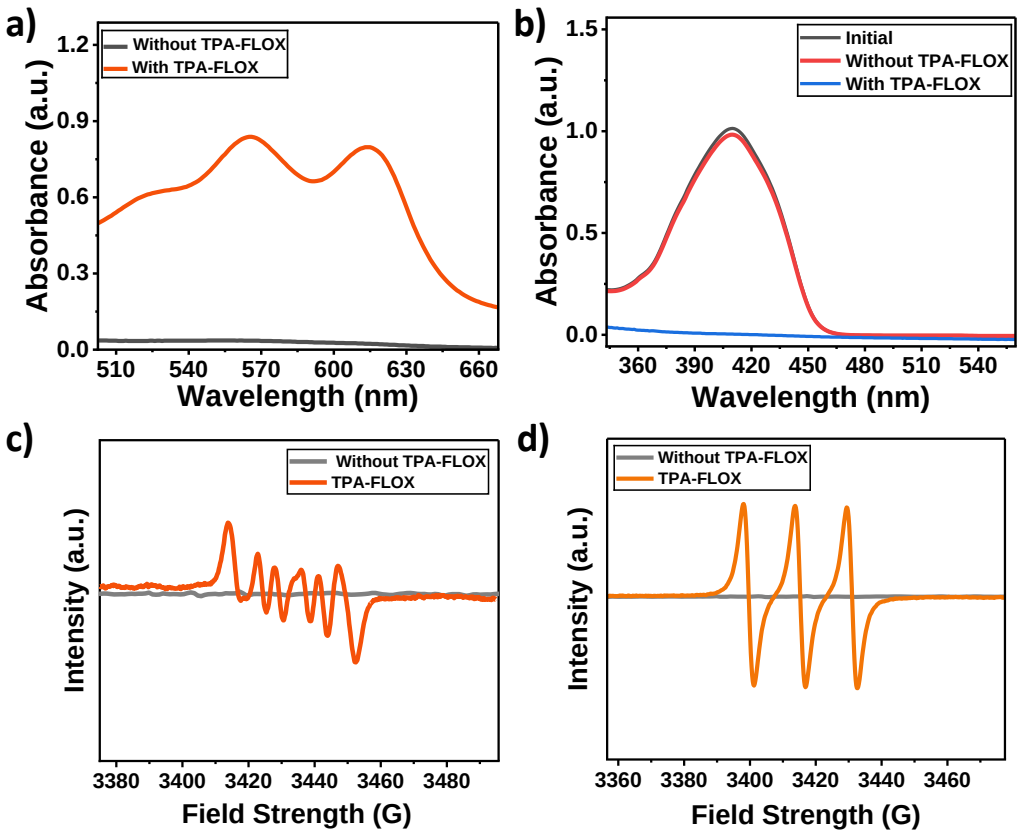

Figure S18. UV–vis absorption spectra of a) TMPD and b) DPBF recorded in the presence and absence of **TPA-FLOX**, and EPR spectra of c) DMPO and d) TEMP obtained under identical conditions. Control experiments performed without the photocatalyst show no appreciable probe response, unambiguously confirming that the observed spectral signals arise solely from photocatalytically generated reactive species in the presence of **TPA-FLOX**.

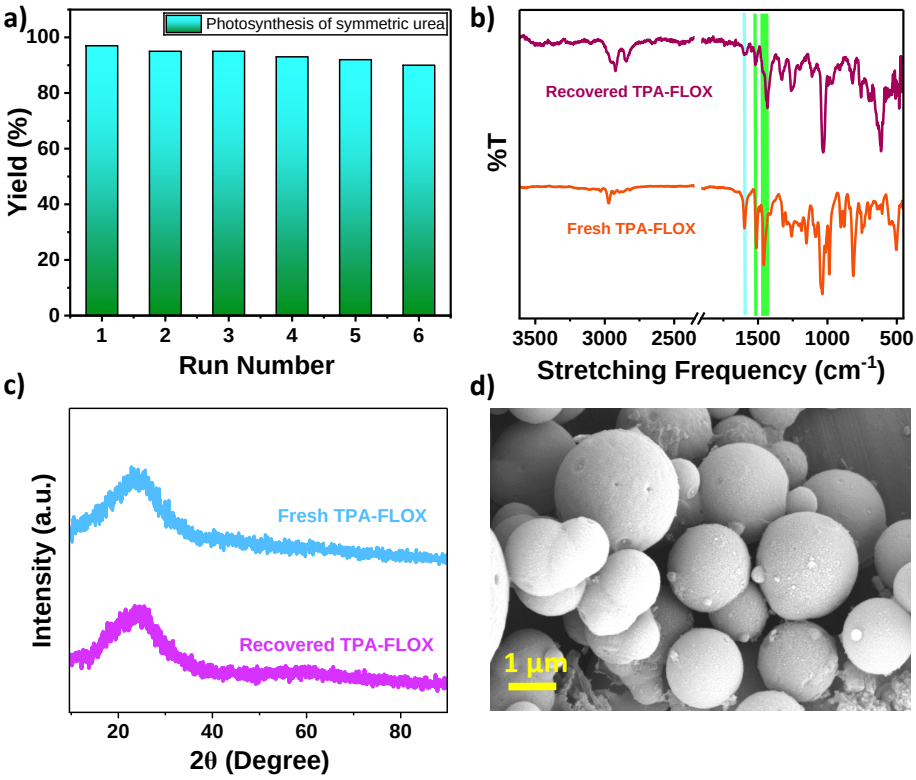

Figure S19. a) Recyclability of **TPA-FLOX** in the photocatalytic synthesis of symmetric urea; b) FTIR spectra and c) PXRD patterns of **TPA-FLOX** after six cycles compared with the fresh sample; d) SEM image of the recovered **TPA-FLOX**.

Table S3: Reaction optimization for the photocatalytic C-3 thiocyanation of indoles[a]

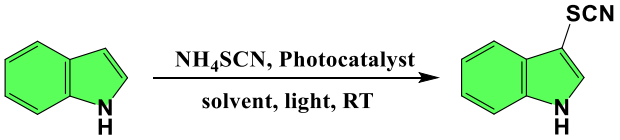

Entry	Substrate	Solvent	Light Source	Time (h)	Yield[b] (%)
1	**TPA-FLOX**	THF	White led	10	99
2	**TPA-FLOX**	MeOH	White led	10	85
3	**TPA-FLOX**	MeOH + acetone	White led	10	88
4	**TPA-FLOX**	THF	Blue led	10	80
5	**TPA-FLOX**	acetone	White led	10	90
6	**TRZ-FLOX**	THF	White led	10	94
7	**TPA-FLO**	THF	White led	10	85

[a]Reaction conditions: Indole (0.2 mmol), NH_4SCN (0.4 mmol), D-A CMPs (5 mg), and solvent (4.0 mL) in a 50 mL Pyrex tube, irradiated with a 24 W white LED under an O_2 atmosphere at room temperature. [b]Isolated yield.

Table S4. Comparison of photocatalytic performance of **TPA-FLOX** in C-3 thiocyanation of indoles with previously reported photocatalysts.

Entry	Photo-catalyst	Catalyst Dosage	Substrate	Light source	Time	Yield	Reference
1	**EDOT–COP**	5 mg	0.2 mmol	6 W blue LEDs	3-10 h	99%	[2]
2	**Cbz–CMP–9**	10 mg	0.25 mmol	14 W LED	4 h	98%	[3]
3	**COF–JLU24**	3 mg	0.3 mmol	30 W blue LED	7 h	95%	[4]
4	**TP–PB COF**	5 mg	0.24 mmol	30 W blue LED (460 nm)	8 h	97%	[5]
5	**PM–PM–COF**	5 mg	0.24 mmol	30 W blue LED (460 nm)	8 h	96%	[6]
6	**MeO–TBT–COF**	5 mg	0.24 mmol	30 W blue LED lamp (460 nm)	8 h	95%	[7]
7	**TPA-FLOX**	5 mg	0.2 mmol	24 W white LED	10 h	99%	This Work
8	**TRZ-FLOX**					94%	
9	**TPA-FLO**					85%	
10	**PAF–405**	5 mg	0.5 mmol	blue LED (420 nm)	10 h	99%	[8]
11	**CMP–CSU6**	20 mg	0.5 mmol	14 W LED (0.20 W/cm^2)	10 h	95%	[9]
12	**0.45%N–ZnO**	0.003 g	0.5 mmol	12 W blue LED	16 h	94%	[10]
13	**Rose Bengal**	1 mol %	0.5 mmol	14 W CFL	18 h	100%	[11]
14	**ARS–TiO2**	7.0 mg, 0.97 μmol g^{-1}	1 mmol	15 W blue LED lamp (λ > 440 nm)	20 h	93%	[12]
15	**$Cs_2AgBiBr_6$**	5 mol%	0.2 mmol	457 nm blue LED	20 h	97%	[13]
16	**SiMo–NDI**	5 mol%	0.5 mmol	White LED (50 W)	24 h	94%	[14]
17	**PDI–COF**	15 mol%	0.4 mmol	100 W white LED (400–750 nm)	48 h	97%	[15]

Table S5. Control experiments for the photocatalytic C-3 thiocyanation of indoles[a]

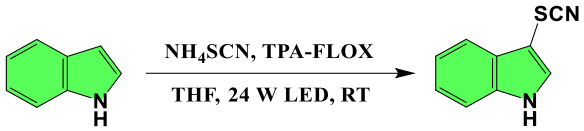

Entry	Reaction Condition	Time (h)	Yield[b] (%)
1	In absence of catalyst	10	10
2	In absence of oxygen	10	18
3	In absence of light	16	trace
4	In presence of KI (hole scavenger)	10	48
5	In presence of $CuSO_4$ (electron scavenger)	10	42
6	In presence of p-BQ ($O_2^{\bullet-}$ scavenger)	10	37
7	In presence of NaN_3 ($^1O_2$ scavenger),	10	40

[a]Reaction conditions: Indole (0.2 mmol), NH_4SCN (0.4 mmol), **TPA-FLOX** (5 mg), and THF (4.0 mL) in a 50 mL Pyrex tube, irradiated with a 24 W white LED under an O_2 atmosphere at room temperature. [b]Isolated yield.

Table S6. Control experiments for the photocatalytic synthesis of 2-benzothiazoles[a]

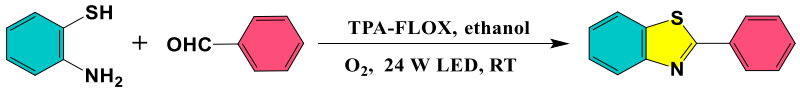

Entry	Condition	Time (h)	Yield[b] (%)
1	**TPA-FLOX**	2	95
2	Without Catalyst	2	27
3	Without light	2	trace
4	Without Oxygen	2	10
5	In presence of NaN_3	2	50
6	In presence of *P*-BQ	2	42
7	In presence of KI	2	53

[a]Reaction condition: 2-aminothiophenol (0.1 mmol), benzaldehyde (0.12 mmol), **TPA-FLOX** (5 mg), and EtOH (3.0 mL) was placed in a 5 mL Pyrex and irradiated with a 24 W white LED under an O_2 atmosphere at room temperature. [b]Yield of isolated product.

Table S7. Comparison of the photocatalytic performance of **TPA-FLOX** in the synthesis of 2-benzothiazoles with previously reported polymer photocatalysts.

Entry	Polymer	Polymer Dosage	Reaction Conditions	Time (h)	Yield (%)	Reference
1	**TAPT-TP-COF**	5 wt%	$NaHCO_3$(2 equiv), EtOH : H_2O (1 : 1), 10 W blue LED, air	10	98	16
2	**CMP-Th-Ph-F**	8 mg	MeOH (2 mL), λ = 450 nm LED, O_2	4	99	17
3	**PAF-406**	3 mg	MeOH (3 mL), 24W blue LED, air	3	99	18
4	**OZBT-COF**	5 mg	MeOH (2 mL), 30 W blue LED, air	3	95	19
5	**TPA-MP-1**	5 mol%	EtOH (1 mL), 24 W blue LED, air	2	86	20
6	**TPA-FLOX**	5 mg	EtOH (3 mL), 24W white LED, O_2	2	95	This work

References

1. L. Duan, P. Zhong, J.-B. Liu, K. Liu and N. Luo, *Mol. Catal.*, 2024, **564**, 114344.
2. W.-K. An, X. Xu, S.-J. Zheng, Y.-N. Du, J. Ouyang, L.-X. Xie, Y.-L. Ren, M. He, C.-L. Fan, Z. Pan and Y.-H. Li, *ACS Catal.*, 2023, **13**, 9845-9856.
3. Z. Deng, H. Zhao, X. Cao, S. Xiong, G. Li, J. Deng, H. Yang, W. Zhang and Q. Liu, *ACS Appl. Mater. Interfaces.*, 2022, **14**, 35745-35754.
4. Z. Li, S. Han, C. Li, P. Shao, H. Xia, H. Li, X. Chen, X. Feng and X. Liu, *J. Mater. Chem. A*, 2020, **8**, 8706-8715.
5. F. Tao, W. Zhou, Z. Li, X. Jiang, L. Wang, Z. Yu, J. Zhang and H. Zhou, *ACS Mater. Lett.*, 2024, **6**, 1120-1129.
6. J. Zhang, F. Tao, W. Wang, C. Gong, Z. Li, W. Zhou, Y. Peng and H. Zhou, *ACS Mater. Lett.*, 2023, **5**, 2799-2806.
7. K. Cai, W. Wang, J. Zhang, L. Chen, L. Wang, X. Zhu, Z. Yu, Z. Wu and H. Zhou, *J. Mater. Chem. A*, 2022, **10**, 7165-7172.
8. Y. He, L. Cao, H. Wang, F. Cui and X. Tao, *Chem. Commun.*, 2025, **61**, 9892-9895.
9. W. Zhang, J. Tang, W. Yu, Q. Huang, Y. Fu, G. Kuang, C. Pan and G. Yu, *ACS Catal.*, 2018, **8**, 8084-8091.
10. M. Hosseini-Sarvari and A. M. Sarvestani, *Photochem. Photobiol. Sci.*, 2021, **20**, 903-911.
11. W. Fan, Q. Yang, F. Xu and P. Li, *J. Org. Chem.*, 2014, **79**, 10588-10592.
12. M. Koohgard, Z. Hosseinpour, A. M. Sarvestani and M. Hosseini-Sarvari, *Catal. Sci. Technol.*, 2020, **10**, 1401-1407.
13. T. Zhong, H. Zhu, Y. Zheng, G. Ren, X. Xie, Q. Fan, Z. Xie and Z.-G. Le, *Chem. Commun.*, 2024, **60**, 4230-4233.
14. W. Dai, C. He, S. Li, Y. Xu, F. Cheng and J.-J. Liu, *Inorg. Chem. Front.*, 2024, **11**, 5185-5195.
15. X. Li, J. Zhou, W. Yin, B. Xie, Z. Liu and J.-J. Liu, *J. Catal.*, 2024, **437**, 115640.
16. Z. Liu, Z. Chen, H. Tong, M. Ji and W. Chu, *Green Chem.*, 2023, **25**, 5195-5205.
17. S. Li, J. Yin, H. Zhang and K. A. I. Zhang, *ACS Appl. Mater. Interfaces.*, 2023, **15**, 2825-2831.
18. J. Shao, H. Wang, X. Tao and G. Zhu, *Chem. Sci.*, 2025, **16**, 13267-13275.
19. W. Wang, Y. Bai, Z. Li, Q. Su, B. Li, M. Lei, J. Feng, A. Xu and Q. Wu, *Chem. Eng. J*, 2024, **501**, 157486.
20. Y. Zhu, S. Li, X. Yang, S. Wang and Y. Zhang, *J. Mater. Chem. A*, 2022, **10**, 13978-13986.